Developing InP SWIR SPAD arrays for an automotive Geiger-mode lidar

Mark Itzler

June 5, 2024

ISSW2024 - The International SPAD Sensor Workshop 2024

InGaAs/InP SWIR SPAD development timeline

- Currently at LUMINAR SEMICONDUCTOR
- This presentation covers work done while at Argo AI (until Jan 2023)

2008 - 2017

First commercial InGaAs/InP **SWIR SPAD cameras** from Princeton Lightwave

Prototype automotive lidar based on SWIR SPAD camera

Princeton Lightwave acquired by ARGO

2018 - 2022

First **SWIR SPAD lidar on an autonomous vehicle**

Lidars **integrated on autonomous vehicle fleets** by Ford and VW

Ford announces **shut-down of Argo**

2023 -

NJ-based **semiconductor device team** moves **to** LUMINAR SEMICONDUCTOR

Presentation Outline

- **Background** of InGaAs/InP SPAD array development for Geiger-mode lidar
- **Lidar system architecture** with quasi-1D SPAD arrays
- SPAD array **design and performance**
- SPAD focal plane array **reliability**
- System performance enhancements: **sliding window oversampling**
- System performance enhancements: **temporal pulse coding**

Legacy SPAD Focal Plane Array: 128 x 32 with 50 μm pitch

- **Initial InP-based SPAD array technology for camera products** from Princeton Lightwave
  - State-of-the-art was 128 x 32 format with 50 μm pixel pitch

Schematic of InP/InGaAs SWIR SPAD

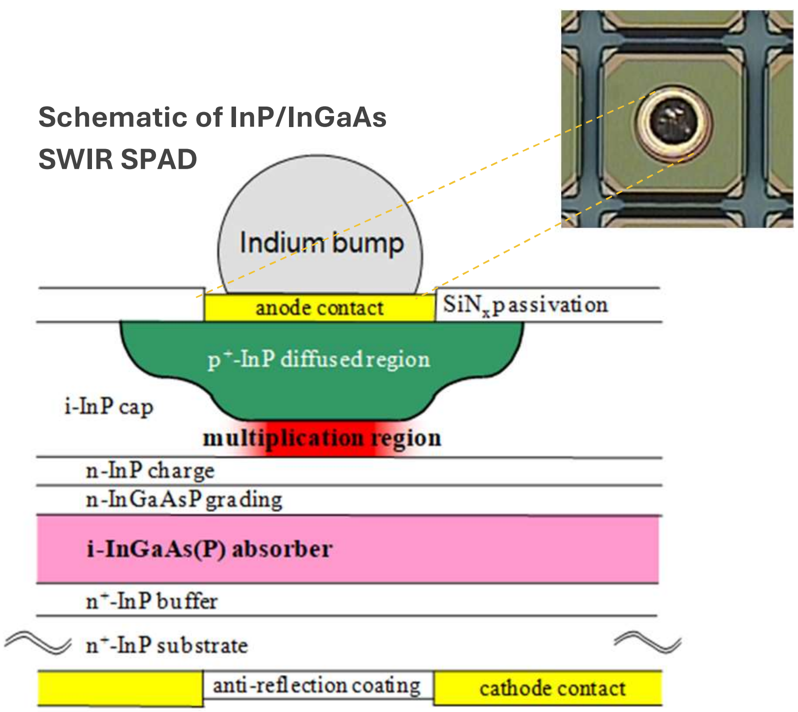

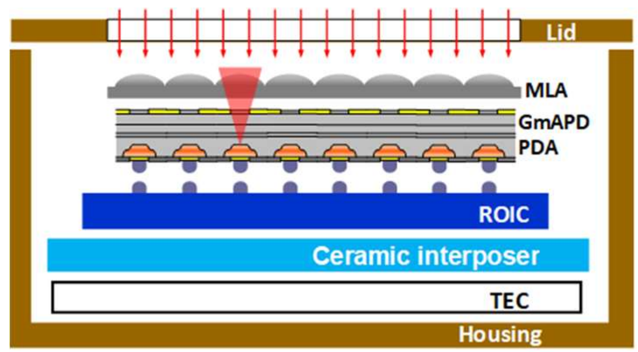

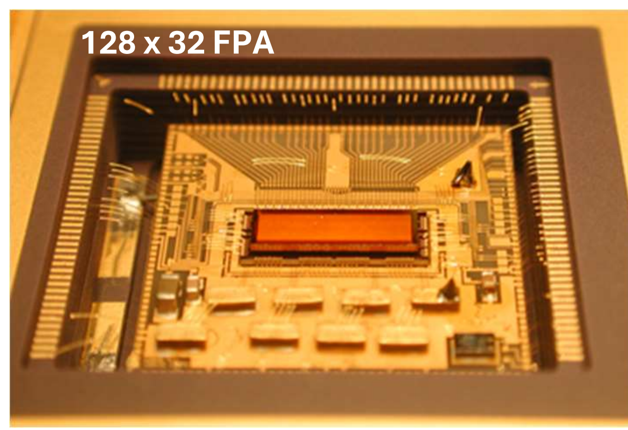

Integrated camera

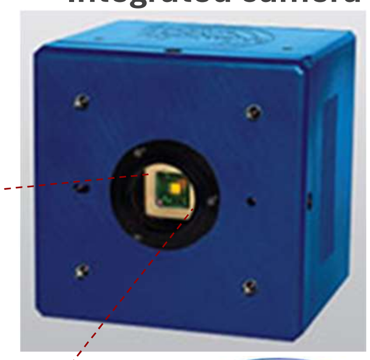

Princeton Lightwave

Digital SPAD detection vs. analog APD detection

- **Single-photon detection** provides “digital” response (“photons to bits”)
  - **Sensitive to single photon returns**
  - **No dependence on number of photons**
  - **Use statistics** to get intensity

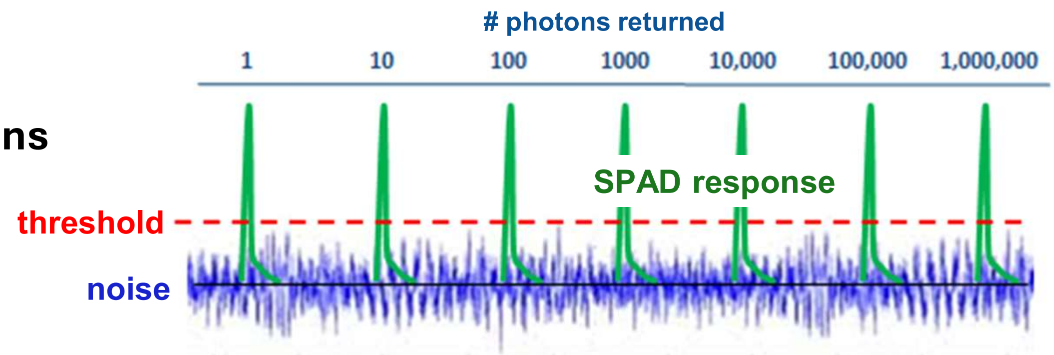

- **Analog detection** using **linear-mode** avalanche photodiodes (APDs)
  - **10s - 100s of photons per return** to overcome noise
  - Output **proportional to number of photons**

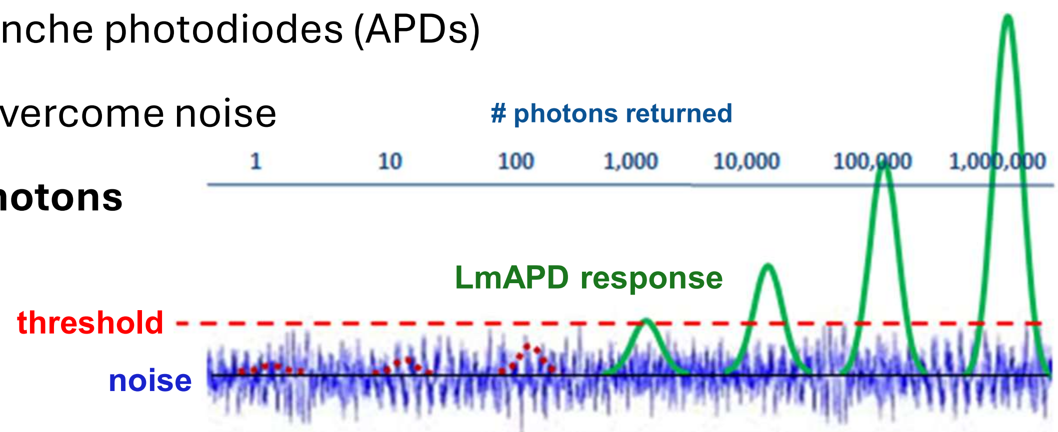

Statistical sampling with Geiger-mode lidar

- **Statistical analysis** of time-of-flight returns with high repetition rate pulses
  - Each point cloud point created from **~100 - 200 samples** (**temporal and spatial**)
  - **Correlated counts** provide high probability of detection for signal returns

Photons incident on lidar receiver aperture, both **reflected signal** and **ambient noise**

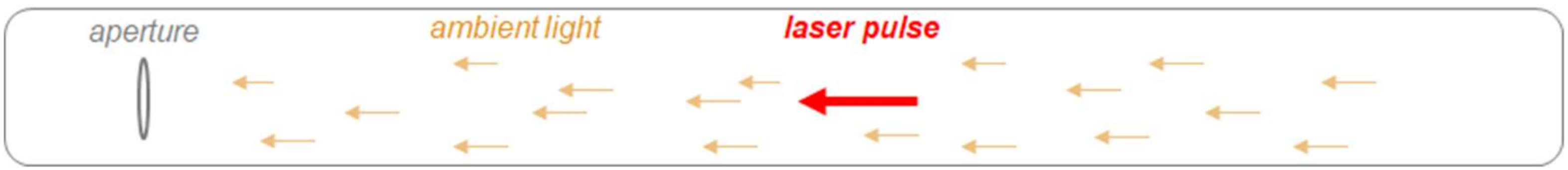

Coincidence processing: build **histogram** of time-of-flight values, **peaks** → **objects reflections**

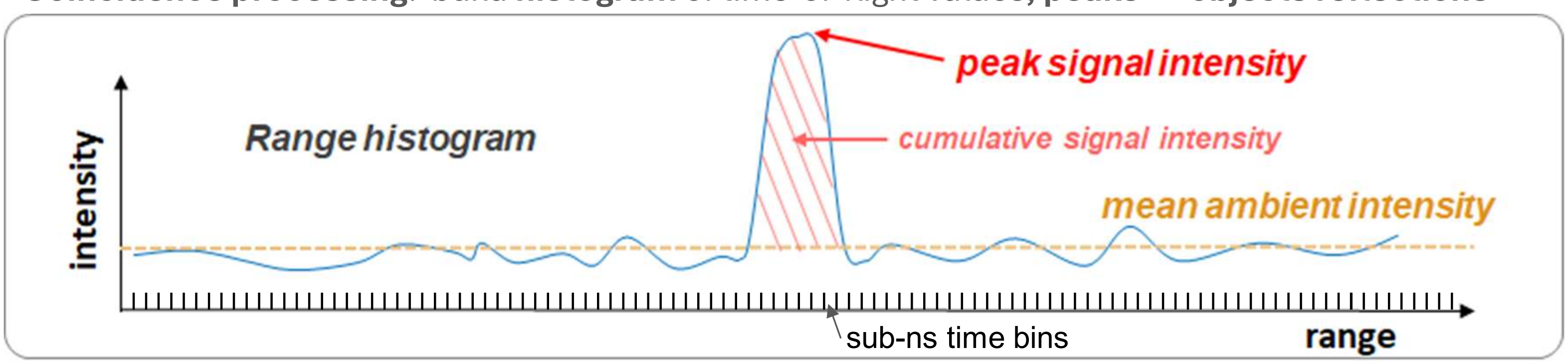

Consecutive lidar frames

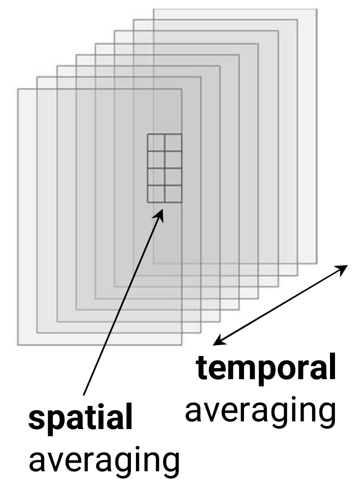

Presentation Outline

- Background of InGaAs/InP SPAD array development for Geiger-mode lidar
- **Lidar system architecture with quasi-1D SPAD arrays**
- SPAD array design and performance
- SPAD focal plane array reliability
- System performance enhancements: sliding window oversampling
- System performance enhancements: temporal pulse coding

Key lidar system requirements for autonomous vehicles

Lidar System Requirements	Implications for Lidar Design & SPADs
360° azimuthal (horizontal) coverage	**Rotating platform** provides 360° with single sensor, **static Tx/Rx path**
Wider **30° vertical FOV at closer range** with **~0.2° x 0.2°** angular resolution	• Use **2 transceivers** optimized for VFOV, resolution, and range • Use **same laser module and SPAD FPA** for both transceivers • **Cover entire VFOV** with laser and SPAD array formats • **Single optical alignment** per transceiver with monolithic arrays
Narrower **10° vertical FOV at longer range** with **~0.1° x 0.1°** angular resolution	
Long-range (~250 m) detection to 10% reflector	
Mid-range (~50+ m) detection to 0.3% reflector	
10 Hz frame rate	Pulse repetition rate for **enough temporal samples** for coincidence processing **while meeting resolution/point density**
Conditions with **high solar flux**	**Wavelength** choice: **good laser transmission** while **attenuating solar background** (which gives upper limit on dark count rate)
Automotive temperature range (e.g., -40°C to +85°C)	**Temperature-stabilize SPAD operation** at higher temperature

Vertical imaging by continuous illumination and detection

- **Cover vertical field of view with fixed 1D arrays:** laser illumination and SPAD array detection
  - Angular resolution determined by receiver optics and detector pixel instantaneous field of view

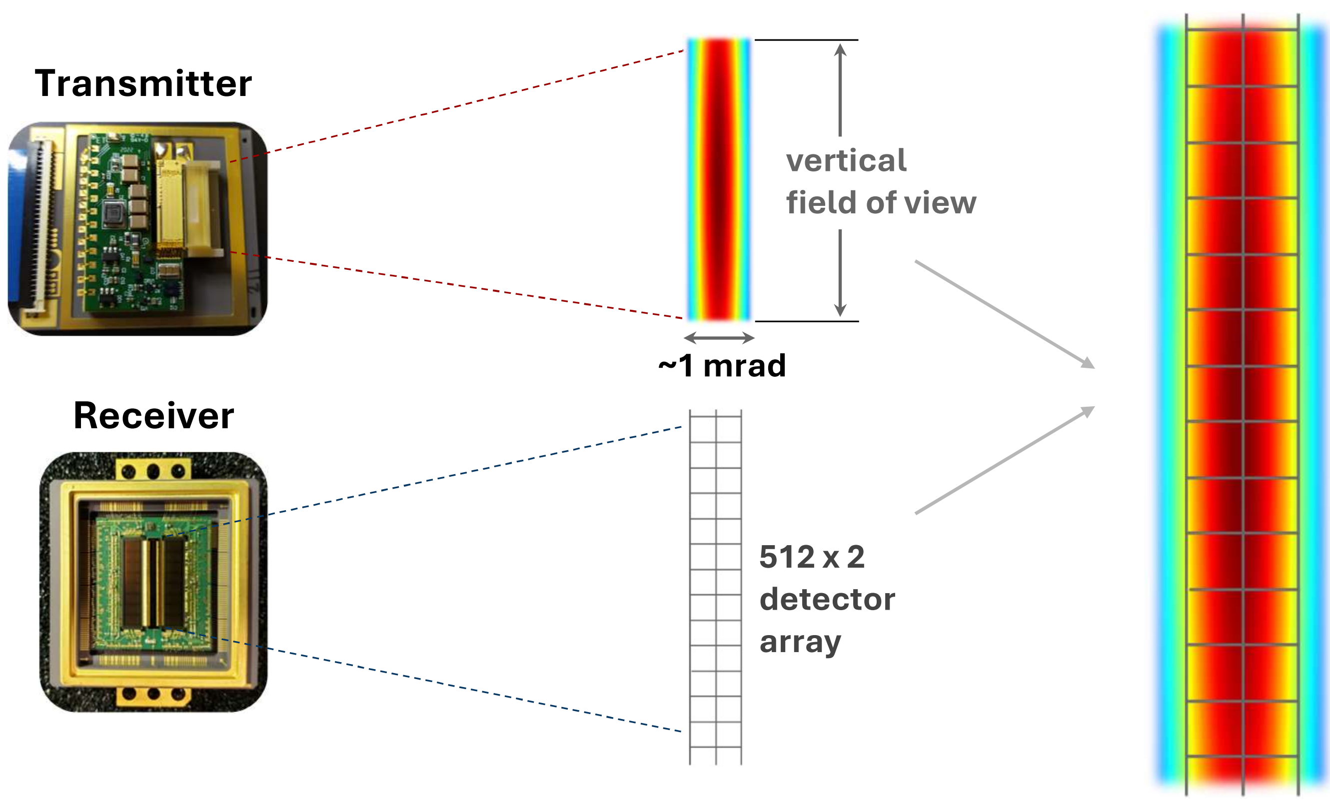

Couple reflected **1D laser illumination** to **quasi-1D detector array**

Use **"super-pixels"** to **optimize trade-off** between **integrated signal** (samples) and **resolution**

Horizontal imaging by high density azimuthal scanning

- **Horizontal space-filling using rotating platform** with high laser pulse rate
  - Average spatially (superpixels) and temporally (multiple pulses) to obtain Geiger-mode samples

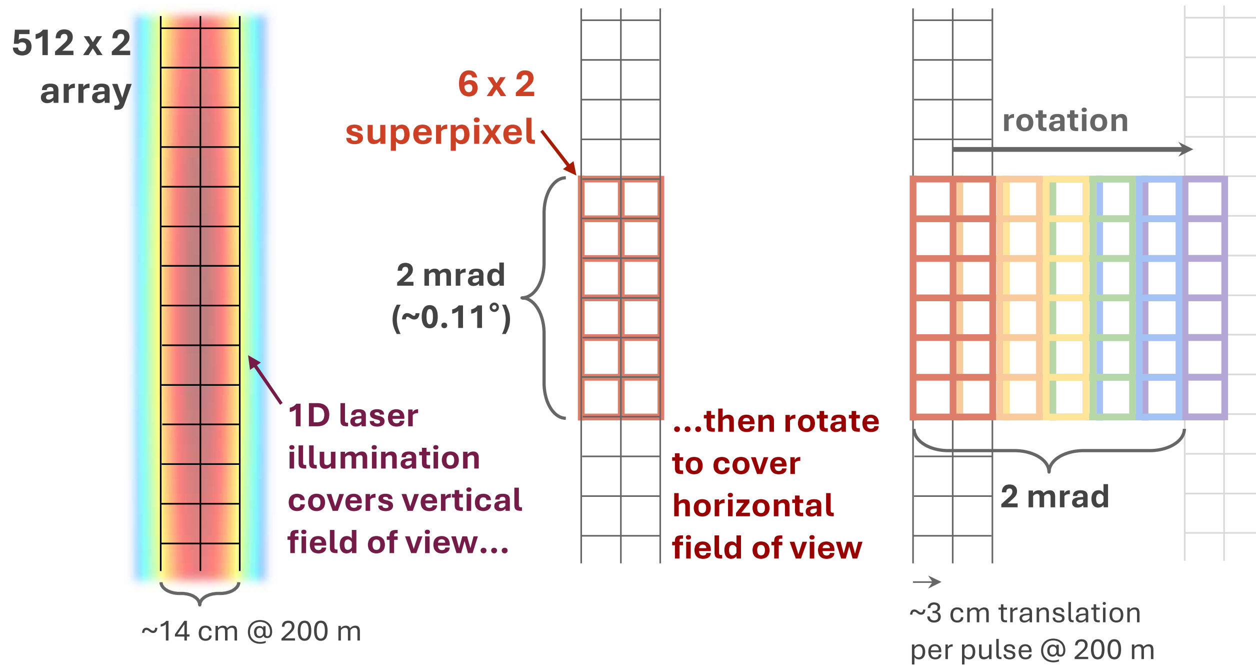

400,000 laser pulses per second

Each color is for a different laser pulse

13 pulses per data frame

LR Transceiver:

12 pixels • 13 pulses = 156 samples to create 1 point cloud point

Point density: 73 pts / deg²

High-level lidar architecture

- Meet requirements using **two independent transceivers** on same rotating platform
  - Mid-range with wider vertical field-of-view (VFOV), long-range with narrower VFOV
  - Point the transceivers in opposite directions (180°) to avoid crosstalk
- Both transceivers use the same Laser Diode Transmitter and SPAD-based Receiver

Mid-range Transceiver

2 m – 75 m
30° VFOV

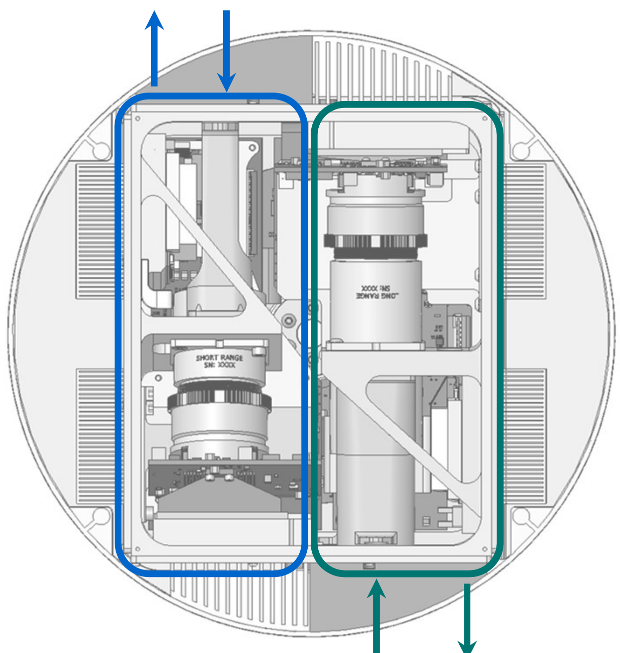

Long-range Transceiver

20 m – 250 m
10° VFOV

Lidar architecture and key assemblies

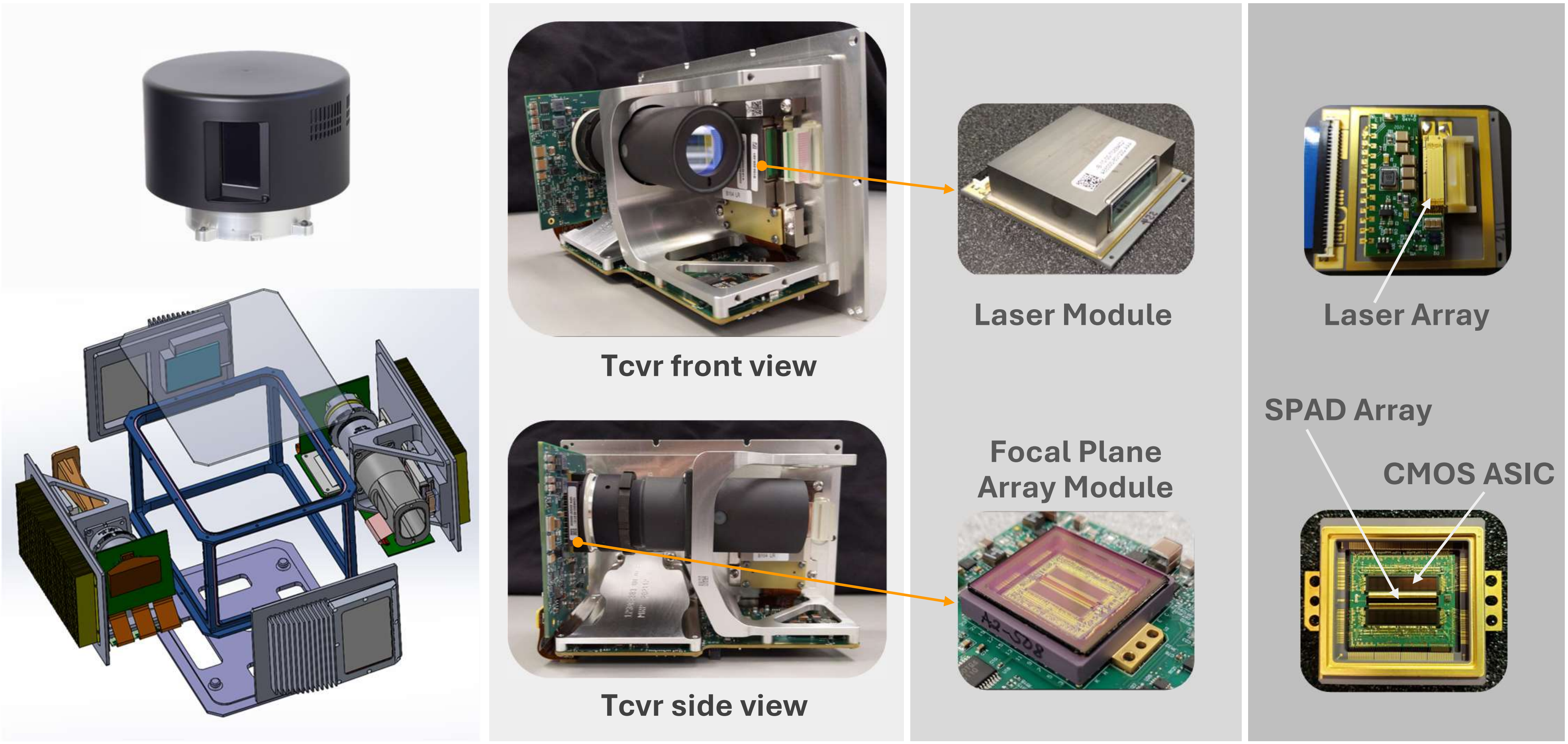

Lidar integration on vehicle

- Lidars were integrated as part of sensor suites including cameras and radar
- ~400 lidars delivered, roughly half for vehicle fleets

On-vehicle point cloud video

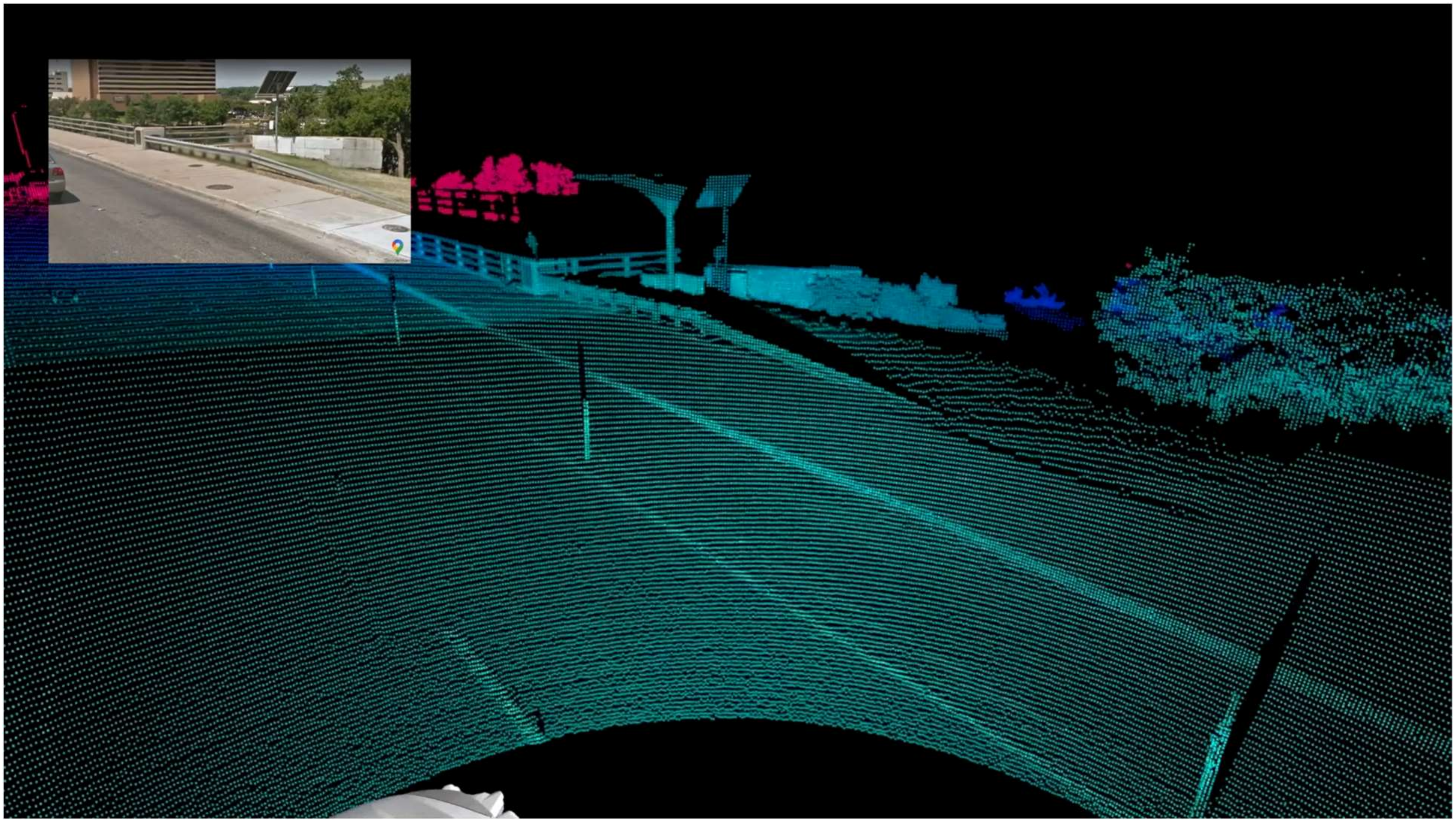

Presentation Outline

- Background of InGaAs/InP SPAD array development for Geiger-mode lidar
- Lidar system architecture with quasi-1D SPAD arrays
- **SPAD array design and performance**
- SPAD focal plane array reliability
- System performance enhancements: sliding window oversampling
- System performance enhancements: temporal pulse coding

SPAD detector design and integration

- Separate Absorption and Multiplication (SAM) InGaAs(P)/InP avalanche diode structure
- Design **512 x 2 SPAD arrays** with reduced **pixel pitch of 25 µm**
- Etched **trenches for pixel isolation** (optical and electrical)
- Sub-micron precision placement of 512 x 2 microlens array aligned to active diameters of <10 µm
- Wire-bonding to two **512 x 1 readout integrated circuits (ROICs)** on either side of 512 x 2 SPAD array

InP/InGaAs SPAD schematic

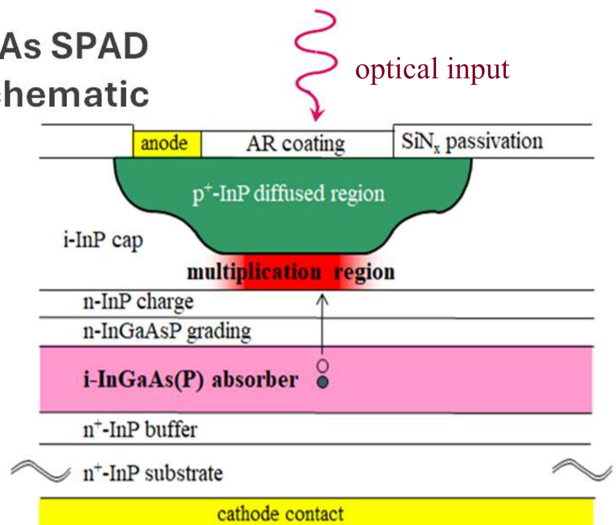

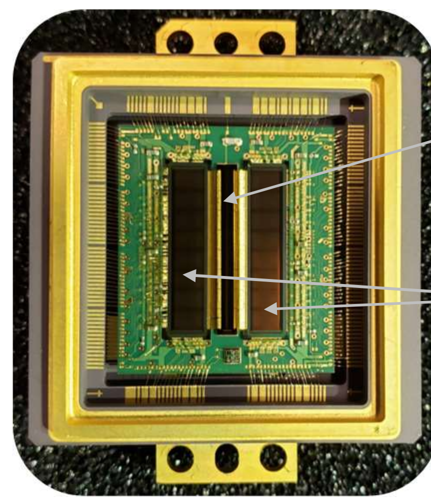

SPAD array

CMOS ROIC

512 x 2 SPAD array performance histograms (25°C)

- DCR and PDE histograms for typical 1024 pixel SPAD array
  - Array was 12.8 mm long → **primary variation due to V_{br} non-uniformity**
- Typical **25°C operation: μ_{DCR} ~ 25 - 35 kHz** at μ_{PDE} ~ 20%

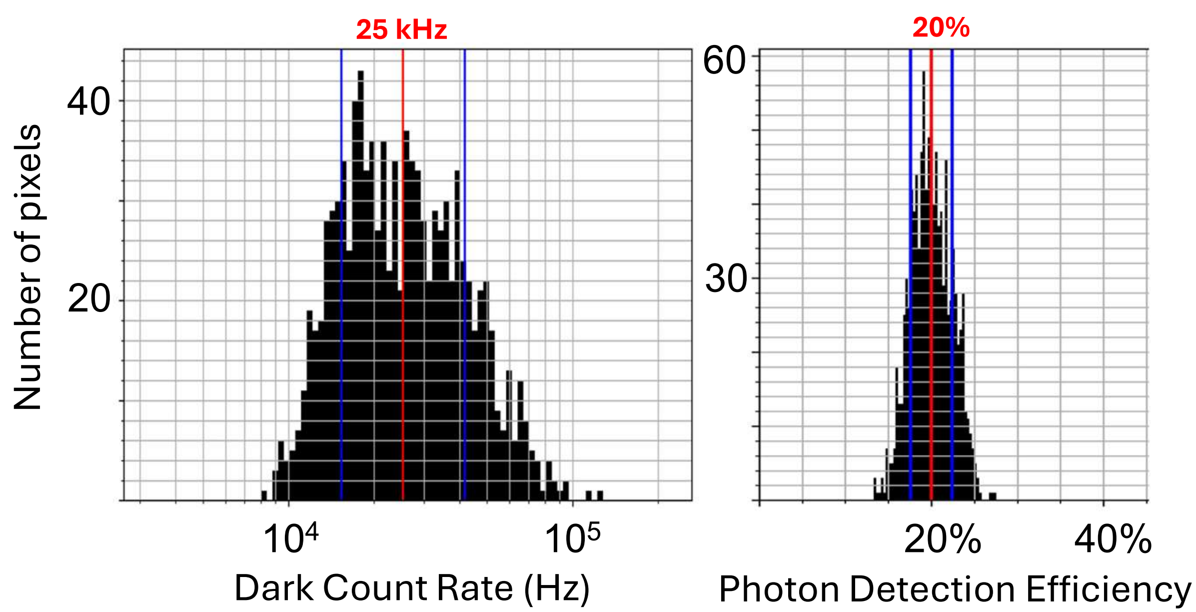

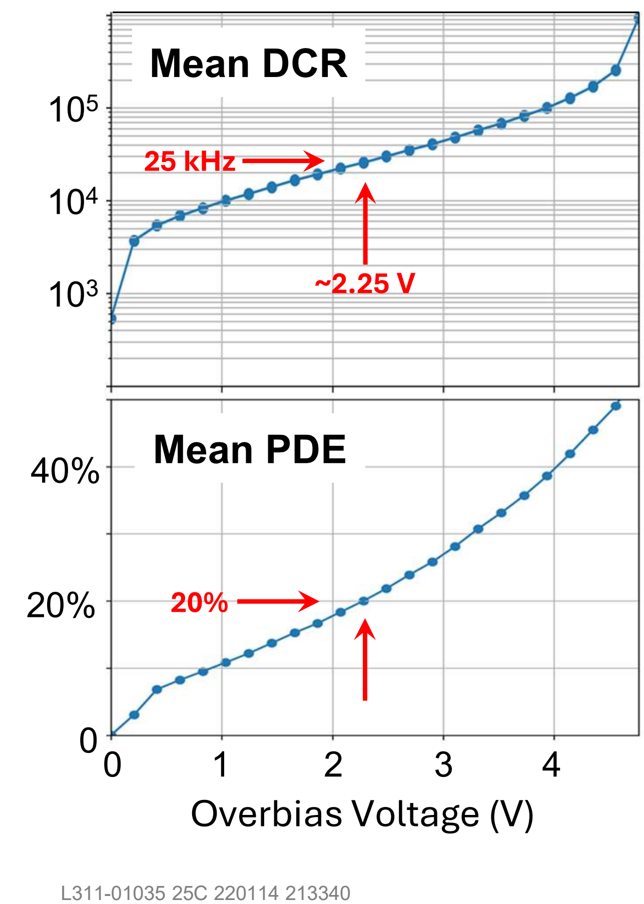

512 x 2 SPAD array spatial distribution of PDE (25°C)

- PDE spatial variation primarily due to breakdown voltage variation
  - **No ROIC-level bias corrections** in 1st generation ROIC

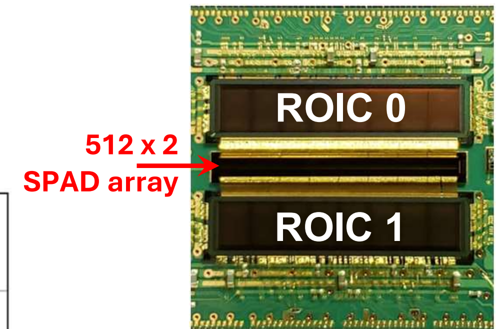

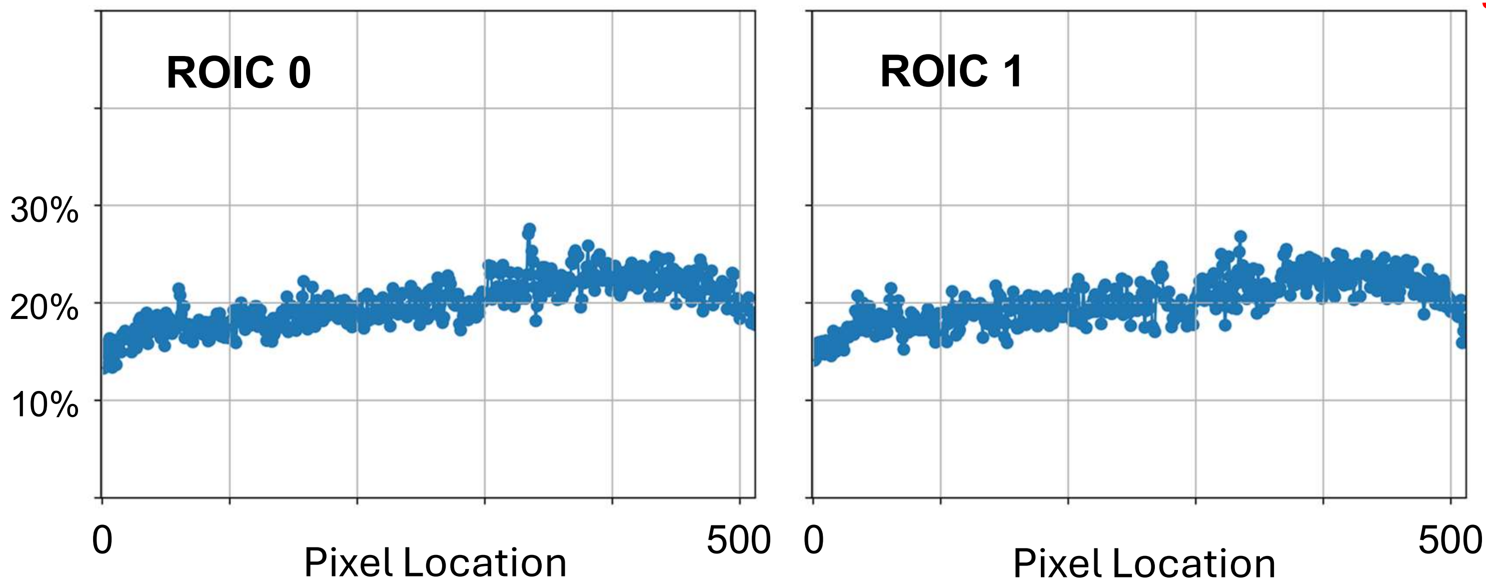

L311-01035 25C 220114 213340

512 x 2 SPAD array performance histograms (**40°C**)

- DCR and PDE histograms for typical 1024 pixel SPAD array
- Typical **40°C operation: μ_{DCR} ~ 60 - 75 kHz**, μ_{PDE} ~ 20%
    - For 100 kHz DCR, ~10% probability of a dark count within 1 μs

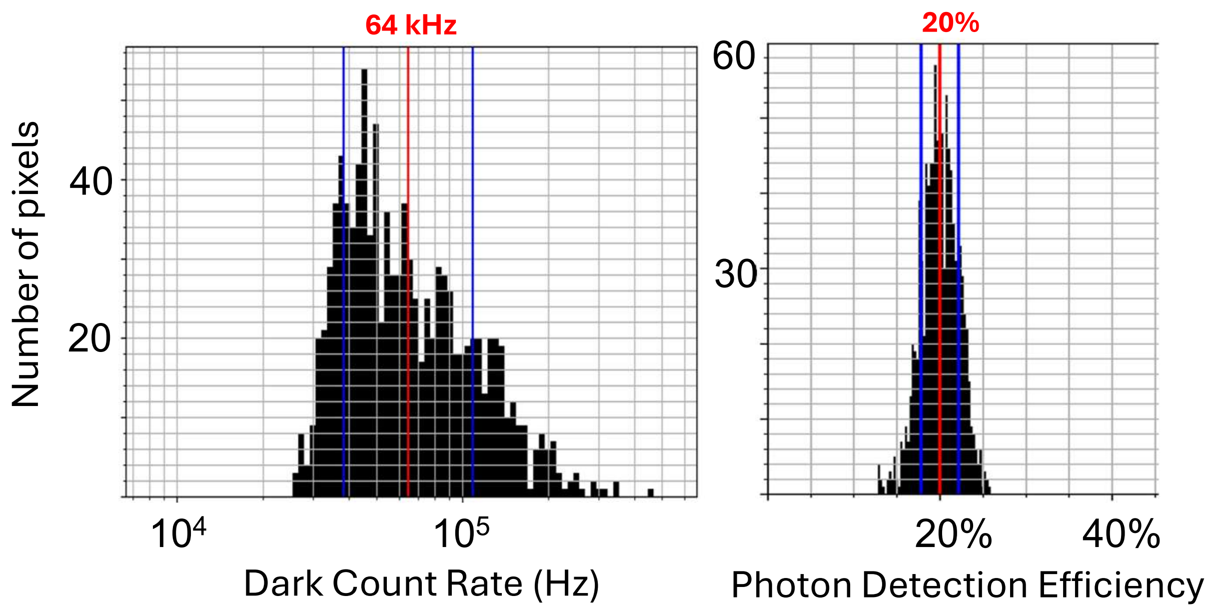

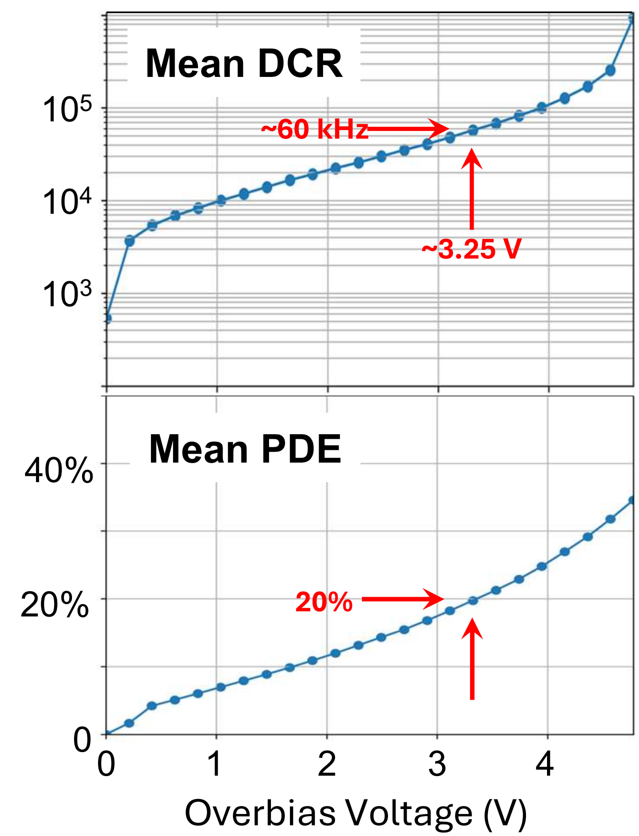

512 x 2 SPAD array spatial distribution of PDE (40°C)

- PDE spatial variation primarily due to breakdown voltage variation
  - No ROIC-level bias corrections in 1st generation ROIC

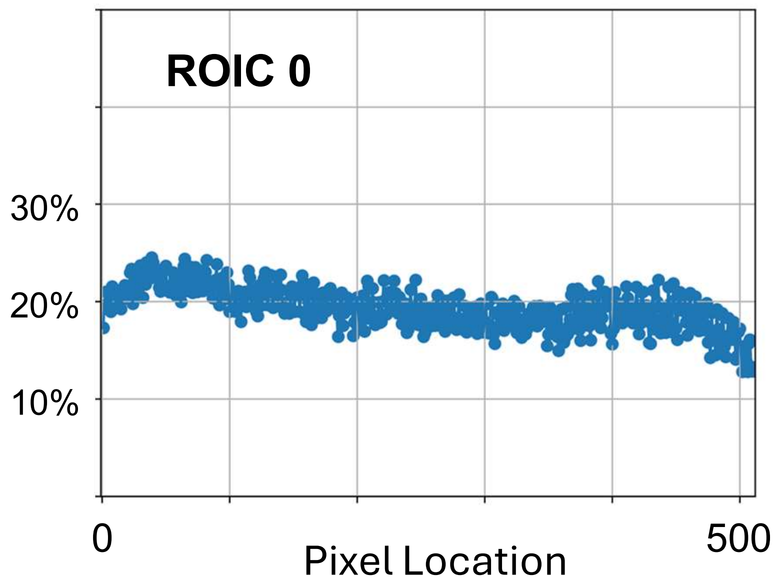

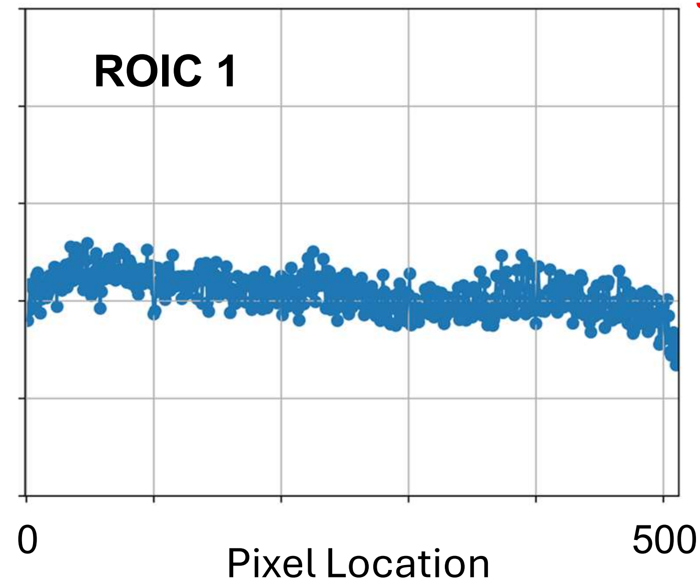

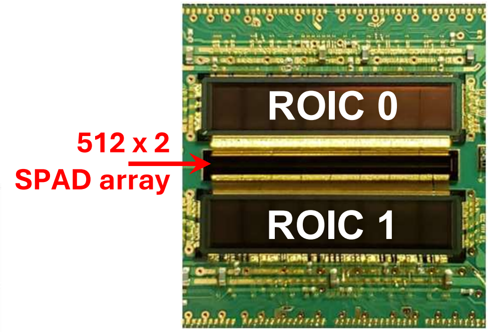

A4-800 40C postseal 220615 172633

Presentation Outline

- Background of InGaAs/InP SPAD array development for Geiger-mode lidar
- Lidar system architecture with quasi-1D SPAD arrays
- SPAD array design and performance
- **SPAD focal plane array reliability**
- System performance enhancements: sliding window oversampling
- System performance enhancements: temporal pulse coding

SPAD focal plane array reliability: 40°C stress

- Initial reliability tests at nominal operating temperature (40°C) and PDE (20%), includes ROICs
  - 1 μs arm/disarm period is ~2X nominal range gate frequency
  - Interval tests are for **average DCR for entire 1024 pixel SPAD focal plane array at 40°C**
- No significant degradation in DCR performance for ~6000 hours

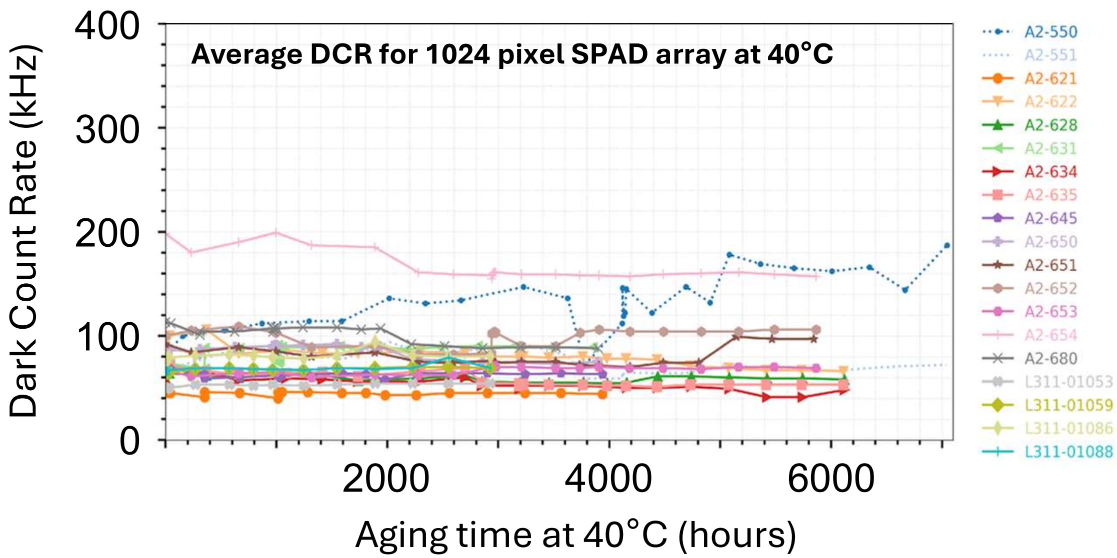

Reliability: 65°C and 85°C stress, 40°C test

- Test included FPAs with range of initial DCR average values for 85°C aging
  - No clear correlation between beginning-of-life DCR and aging behavior
- **85°C stress found to have ~13X acceleration factor relative to 40°C stress**
  - Aging **acceleration assessed by analysis of voltage margin below DCR runaway** at high bias

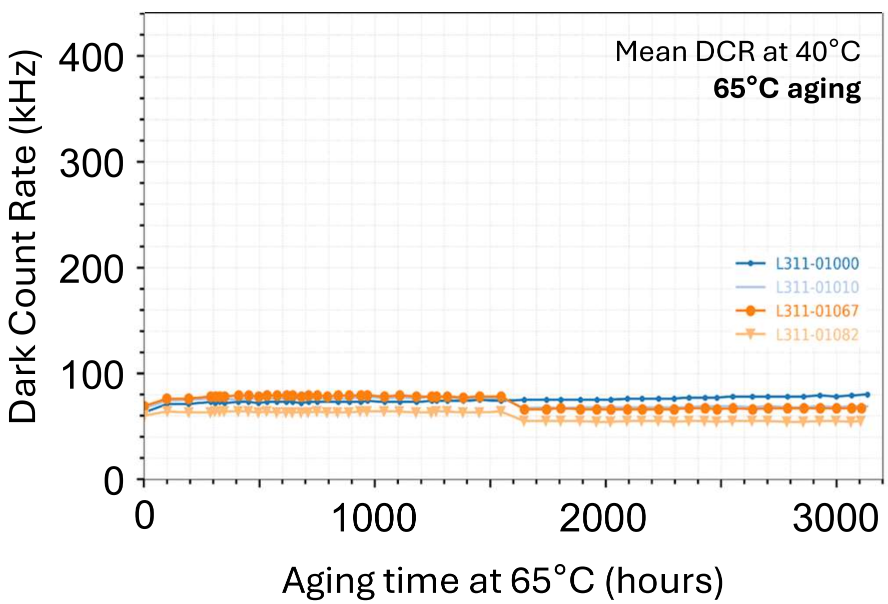

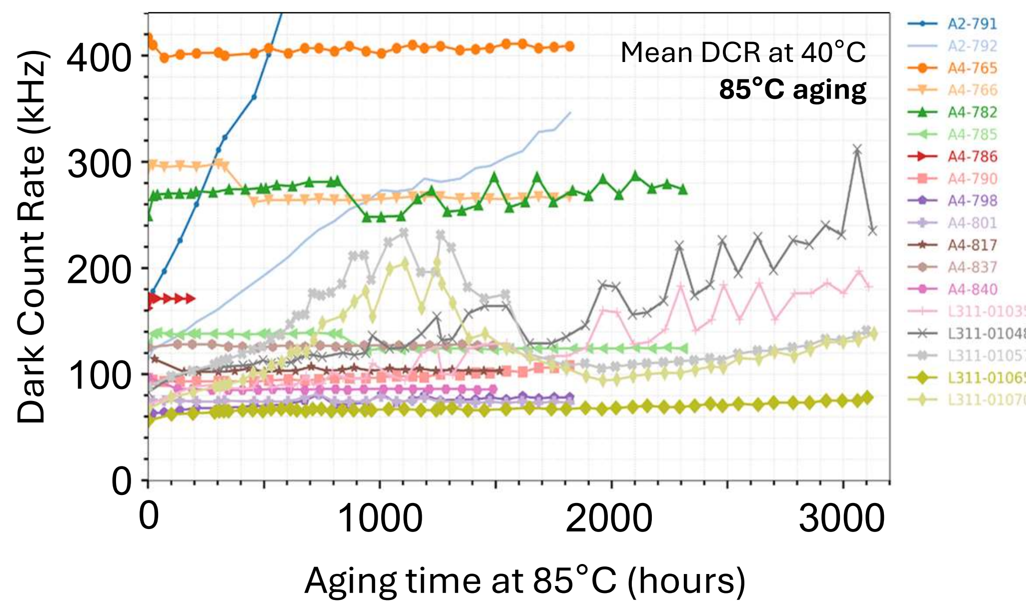

Reliability Summary

- No systematic degradation of DCR for aging at 40°C (6000 hrs) and 65°C (3000 hrs)
- Initial evidence of DCR degradation with 85°C aging by 3000 hours
  - **Acceleration factor** estimated from **voltage margin below DCR runaway**
  - **13X acceleration from 40°C to 85°C** → effective activation energy **E_a ~ 0.55 eV**
  - E_a ~ 0.7 – 0.8 eV for discrete SPADs aged at fixed bias and higher temp (150°C – 200°C)
- **Worst-case lifetime estimate: ~40,000 hrs (at 40°C)** from ~3000 hrs (at 85°C) x 13
  - Comfortably exceeded lidar mission profile of ~10K – 20K hours operation
  - Could increase lifetime by 2X per 10°C decrease (but more power dissipation)
- Small fraction (~5%) of FPAs exhibited early degradation
  - **Manufacturing maturity and screening methods** would be key to eliminating early degradation

Presentation Outline

- Background of InGaAs/InP SPAD array development for Geiger-mode lidar
- Lidar system architecture with quasi-1D SPAD arrays
- SPAD array design and performance
- SPAD focal plane array reliability
- **System performance enhancements: sliding window oversampling**
- System performance enhancements: temporal pulse coding

Resolution enhancement with oversampling

- For Geiger-mode histogramming, use clusters of neighboring pixels for single point cloud point
- **Default scheme: non-overlapping windows** along vertical direction of SPAD array
- **Oversampling: overlap sliding windows** → data extraction at **native pixel resolution**
  - Key benefit: **exploits spatial correlations** at native pixel resolution
  - Can implement selectively using same raw data, e.g., in specific regions of interest
- **Azimuthal oversampling** to increase point density in horizontal direction

Default superpixel sliding window

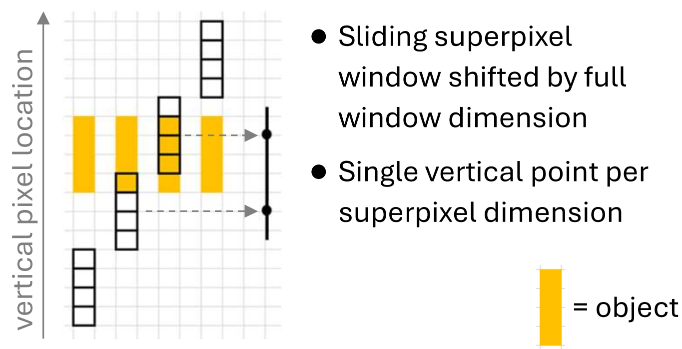

- Sliding superpixel window shifted by full window dimension
- Single vertical point per superpixel dimension

Higher resolution oversampling scheme

- Can provide point density at native pixel density

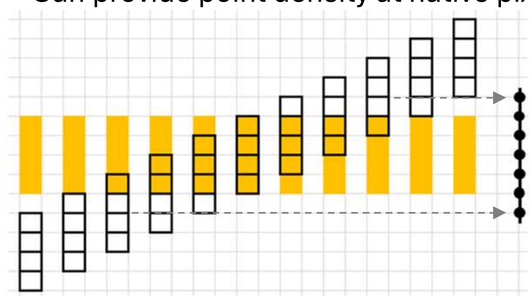

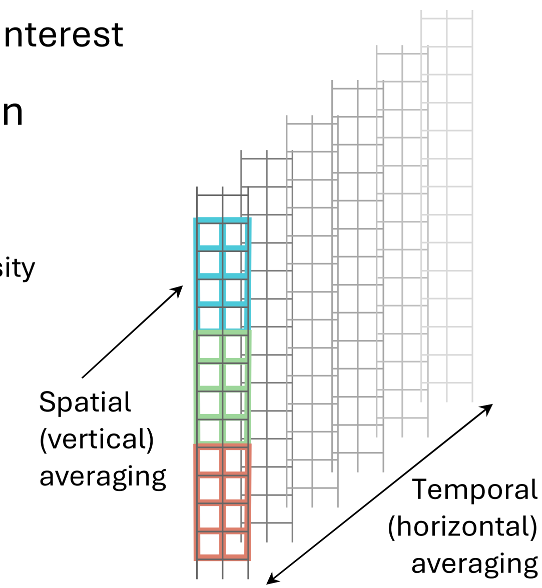

Earlier literature on oversampling with windowing

- Use **oversampling** to extract **information at length scales smaller than point spread function**
  - "Sub-volume" information can be recovered from larger imaging window using multiple sliding window samples

Radar range oversampling (2005)

228 JOURNAL OF ATMOSPHERIC AND OCEANIC TECHNOLOGY VOLUME 23

Resolution Enhancement Technique Using Range Oversampling

TIAN-YOU YU
School of Electrical and Computer Engineering, University of Oklahoma, Norman, Oklahoma

GUIFU ZHANG
School of Meteorology, University of Oklahoma, Norman, Oklahoma

ANIL B. CHALAMALASETTI
School of Electrical and Computer Engineering, University of Oklahoma, Norman, Oklahoma

RICHARD J. DOVIAK AND DUSAN ZRNIĆ
NOAA/National Severe Storms Laboratory, Norman, Oklahoma

(Manuscript received 19 January 2005, in final form 12 July 2005)

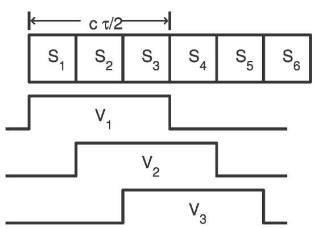

FIG. 1. A schematic diagram of L (=3) range oversampling. Each oversampled signal $V_i(t)$ consists of independent signals from L subvolumes (S_i to S_{L+i-1}).

$$\begin{bmatrix} V_1(t) \\ V_2(t) \\ V_3(t) \end{bmatrix} = \begin{bmatrix} 1 & 1 & 1 & 0 & 0 \\ 0 & 1 & 1 & 1 & 0 \\ 0 & 0 & 1 & 1 & 1 \end{bmatrix} [S_1(t) S_2(t) S_3(t) S_4(t) S_5(t)]^T.$$

Optical coherence tomography lateral over-sampling (2017)

Research Article Vol. 8, No. 3 | 1 Mar 2017 | BIOMEDICAL OPTICS EXPRESS 1319

Biomedical Optics EXPRESS

Lateral resolution improvement of oversampled OCT images using Capon estimation of weighted subvolume contribution

EVGENIA BOUSI,[1] IOANNA ZOUVANI,[2] AND COSTAS PITRIS[1,*]
[1]*KIOS Research Center, Department of Electrical and Computer Engineering, University of Cyprus, Nicosia, Cyprus*
[2]*Nicosia General Hospital, Nicosia, Cyprus*

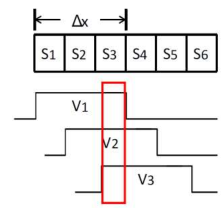

Fig. 1. A schematic diagram of L = 3 lateral oversampling. Each oversampled signal Vi consists of independent signals from L subvolumes (S_i to S_{L+i-1}) with a 2/3 overlap between volumes which share signals Si to S_{L+i-2} with the previous volume [15]. The red rectangle indicated the shared volume which can be isolated from appropriately combining the oversampled signals.

$$\begin{bmatrix} V_1(t) \\ V_2(t) \\ V_3(t) \\ \vdots \\ V_L(t) \end{bmatrix} = \begin{bmatrix} a_1 & \dots & a_L & 0 & 0 & 0 & 0 & 0 \\ 0 & a_1 & \dots & a_L & 0 & 0 & 0 & 0 \\ 0 & 0 & a_1 & \dots & a_L & 0 & 0 & 0 \\ \vdots & & & & & & & \vdots \\ 0 & 0 & 0 & 0 & 0 & a_1 & \dots & a_L \end{bmatrix} [S_1(t) \quad S_2(t) \quad S_2(t) \quad \dots \quad S_{2L-1}(t)]^T$$

High resolution with oversampling: close range

- Oversampling provided 3072 x 512 image for 60° x 10° swath
  - **0.02° x 0.02° angular resolution** with 50 ms acquisition time

Lidar data colored by range and shaded by intensity

Camera image for reference

High resolution with oversampling: long range

- 512 x 512 image for 10° x 10° swath with 0.02° x 0.02° resolution in 8 ms
  - Sufficient resolution for **dozens of points on a pedestrian at 200 m**

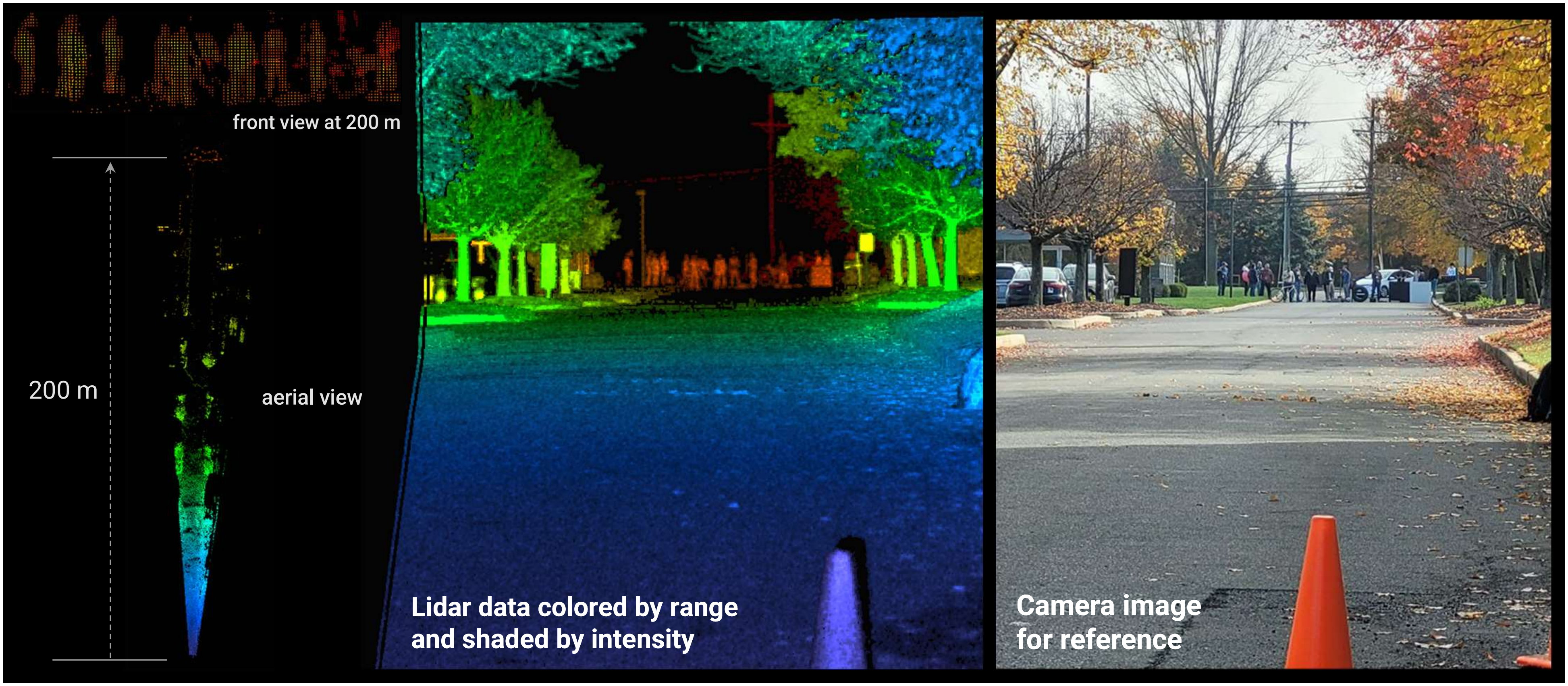

Presentation Outline

- Background of InGaAs/InP SPAD array development for Geiger-mode lidar
- Lidar system architecture with quasi-1D SPAD arrays
- SPAD array design and performance
- SPAD focal plane array reliability
- System performance enhancements: sliding window oversampling
- **System performance enhancements: temporal pulse coding**

Range ambiguity with periodic lidar range gates

- **Range ambiguity due to aliasing effects** resulting from reflections beyond the maximum range R_{rg} of a lidar range gate duration

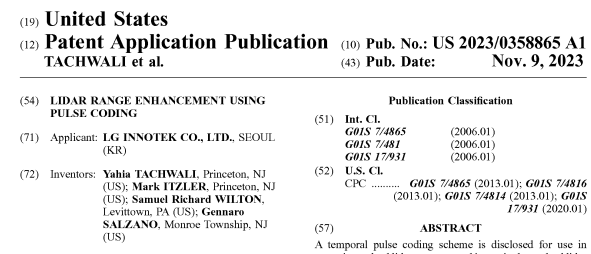
(19) United States
(12) Patent Application Publication (10) Pub. No.: US 2023/0358865 A1
TACHWALI et al. (43) Pub. Date: Nov. 9, 2023

(54) LIDAR RANGE ENHANCEMENT USING PULSE CODING

(71) Applicant: LG INNOTEK CO., LTD., SEOUL (KR)

(72) Inventors: Yahia TACHWALI, Princeton, NJ (US); Mark ITZLER, Princeton, NJ (US); Samuel Richard WILTON, Levittown, PA (US); Gennaro SALZANO, Monroe Township, NJ (US)

Publication Classification

(51) Int. Cl.
G01S 7/4865 (2006.01)
G01S 7/481 (2006.01)
G01S 17/931 (2006.01)

(52) U.S. Cl.
CPC G01S 7/4865 (2013.01); G01S 7/4816 (2013.01); G01S 7/4814 (2013.01); G01S 17/931 (2020.01)

(57) ABSTRACT

A temporal pulse coding scheme is disclosed for use in

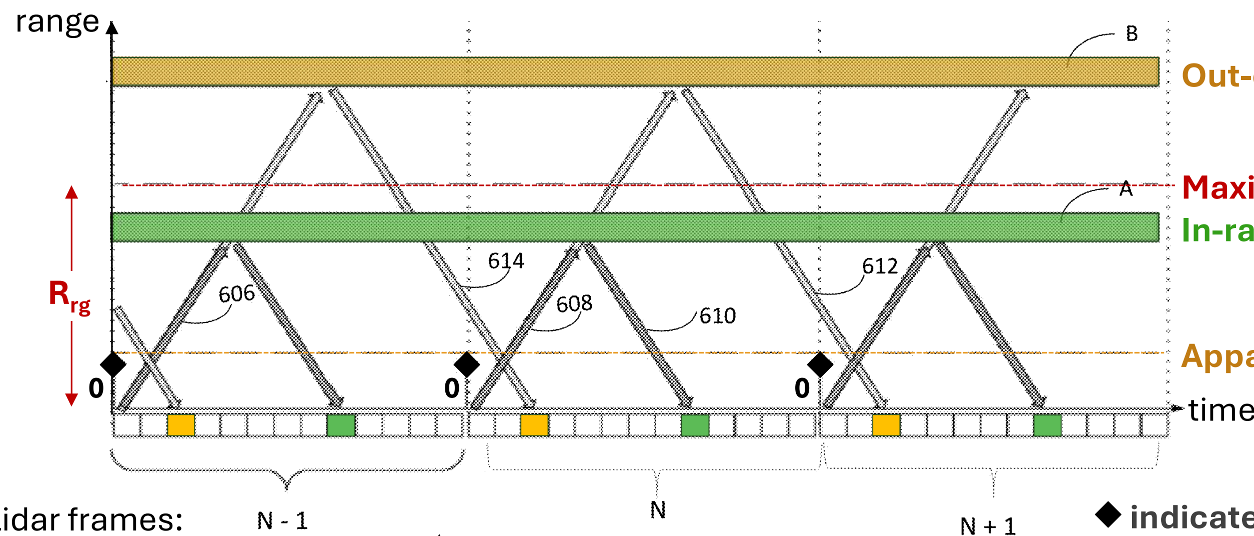

Out-of-range object

Maximum range gate distance

In-range object

Apparent distance of out-of-range object

Three lidar frames:

◆ **indicates time of laser pulse emission**

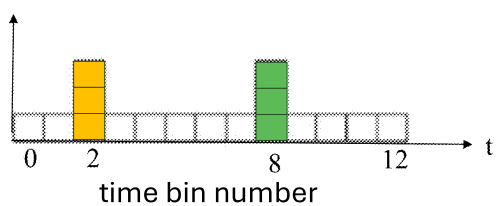

Pulse coding using laser pulse timing offsets

- For **data frame of P pulses**, introduce **sequence of pulse timing offsets**
- **Decode for 0^{th} order range returns by subtracting pulse offset** within a given lidar frame
  - For appropriate offset sequence, higher order returns are spread out to only one count per time bin
- To **decode for N^{th} order range returns**, use N^{th} cyclic variation of 0^{th} order code

Example of cyclic pulse code [1, 3, 0] for every three lidar frames

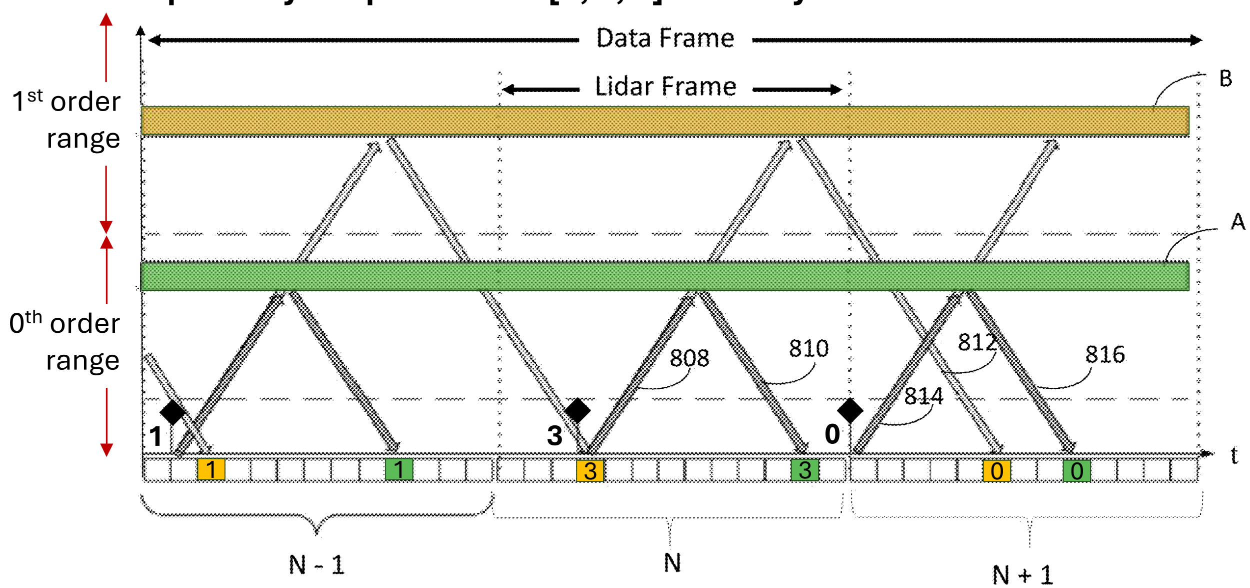

◆ indicates laser pulse timing (number is offset in bins)

0^{th} order decoding sequence [1, 3, 0]

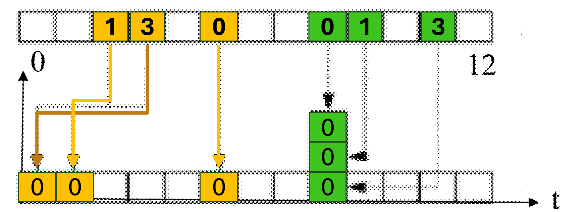

1^{st} order decoding by cyclic variation: [1, 3, 0] → [0', 1', 3']

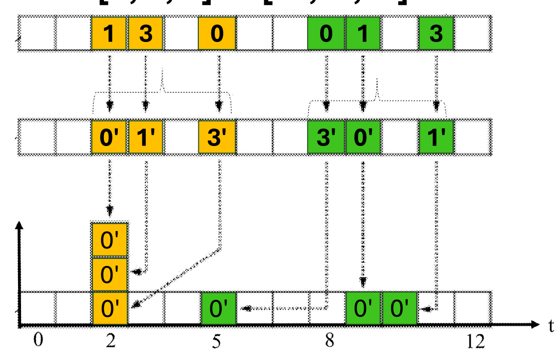

Summary of Cyclic Pulse Coding

- Temporal offset pulse coding **eliminates range aliasing effects**
  - Returns outside target range gate do not coincide after decoding
  - 0^{th} order code extracts returns in 0^{th} order range $(0, R_{rg})$
- Pulse coding **provides dramatic range enhancement**
  - Set of P pulses measure returns to distance $P \cdot R_{rg}$
  - N^{th} order cyclic permutation of 0^{th} order code extracts returns from N^{th} order range $(N \cdot R_{rg}, (N+1) \cdot R_{rg})$
- Effectively allows use of **multiple pulses in flight** at the same time
- Ideally suited to Geiger-mode lidar
  - **Coincidence processing already incorporates P pulses** per resolution element
- Can also make use of receiver range gate timing to enhance long-range detection
  - **Delay arming of range gate** to favor detection of objects at longer ranges

SWIR SPAD-based lidar summary

- **SPAD-based rotating two-transceiver lidar** sensor design for AV fleets
- Employed **512 x 2 quasi-1D SPAD arrays** coupled to **laser diode line illumination**
- Pilot production volumes showed **good SPAD performance and array uniformity**
- SPAD-based **focal plane array reliability shown to meet AV mission profile**
- **Oversampling techniques** applied to Geiger-mode data shown to **increase resolution by 25X**
- **Pulse coding eliminated range ambiguity effects** and provided **dramatic range enhancement**

- **AV fleets have different needs (and business models)** than consumer vehicles
  - Roof-mounted rotating lidar not desirable for consumer vehicles, but effective for AV fleets
- Architecture impact on **cost**: it's **not about InGaAs** – it's the **large-format arrays**
  - Significant further pitch reduction necessary to address cost reduction with this architecture

Acknowledgment

These results are the output of an incredible team of scientists and engineers that I have worked with for many years.

I'm grateful to all of my former colleagues who made this work possible at Argo AI and Princeton Lightwave.

Thank you!

LUMINAR SEMICONDUCTOR

Thank you!